X-611-64-345

NASA TMX-55152

AN EXPERIMENTAL EXAMINATION OF LOW-ENERGY COSMIC RAY HEAVY NUCLEI

BY

C. E. FICHTEL
D. E. GUSS
K. A. NEELAKANTAN

NOVEMBER 1964

GODDARD SPACE FLIGHT CENTER

GREENBELT, MARYLAND

An Experimental Examination of Low-Energy Cosmic Ray Heavy Nuclei

C. E. Fichtel, D. E. Guss, and K. A. Neelakantan*
Goddard Space Flight Center, Greenbelt, Maryland

ABSTRACT

19714 over

In a sounding rocket experiment flown from Fort Churchill on September 4, 1963, a finite flux of cosmic ray nuclei with charges greater than that of helium was detected at energies below the experimental energy cutoff of balloon-borne experiments. The particles were examined by extending large sheets of nuclear emulsions from the sides of the rocket during its period outside the atmosphere. The flux of medium nuclei ($6 \leq Z \leq 9$; Z = nuclear charge) in the energy range from 30 to 150 MeV/nucleon was measured as $0.67 \pm .13$ particles/(m^2 sr sec), and the flux of ($10 \leq Z \leq 19$) nuclei in the energy range from 40 to 190 MeV/nucleon was $0.31 \pm .09$ particles/(m^2 sr sec). A finite flux of light nuclei ($3 \leq Z \leq 5$) also was seen in the 30 to 110 MeV/nucleon region. The abundances of medium and ($10 \leq Z \leq 19$) nuclei relative to helium nuclei in the same energy intervals were found to be significantly less than the relative abundances previously determined at high energies. However, within the statistical uncertainty, the relative differential flux values observed in the vicinity of the earth are consistent with the helium, medium, and ($10 \leq Z \leq 19$) nuclei having the same source

[redacted]

spectrum at least above about 0.2 BeV/nucleon for a wide range of source spectral shapes and an interstellar path length of the order of those normally assumed (i.e., 2.5 g/cm^2 or slightly larger). Other possible interpretations also are considered.

INTRODUCTION

Over the last decade the study of cosmic radiation has progressed considerably and has reached the point where the fundamental properties are becoming reasonably well established.[1-3] The proton energy spectrum now is being measured from 0.01 BeV/nucleon to approximately 10^{10} BeV/nucleon, and the composition of the cosmic radiation has been measured numerous times in the energy region above approximately 0.2 BeV/nucleon. In this region, the composition appears to be independent of energy, at least up to about 10^6 BeV/nucleon, with the possible exception of a small relative increase of the light nuclei in the 0.2 to 0.5 BeV/nucleon interval.[4-8] In particular, the helium to medium nuclei and the helium to heavy nuclei ratios are known to be the same to within about a 15% experimental uncertainty in the region from 0.3 to 7.5 BeV/nucleon. The data also have revealed that there is a strong modulation of the cosmic radiation which is fairly certainly associated with the solar cycle. In the measured energy interval, the variation of cosmic ray intensity is greatest at the lowest energies.[9]

In an effort to increase our general experimental knowledge of the cosmic radiation and at the same time obtain some new insight into some of these questions, an experiment was undertaken to examine the intensity of the heavier nuclei in the cosmic radiation in the region below about 0.2 BeV/nucleon. The first question to be answered was whether or not there are any medium or heavy nuclei in this low-energy region. A cosmic ray source with a very high energy threshold for acceleration of the high charges could create a near absence of these particles, since only some particles which have been degraded in energy in their interstellar travels would be present. However, if particles are present, the measurement of their properties can provide some restraints on the combined questions of the interstellar travel of cosmic rays and the spectra at the origin.

The local solar modulation has the same effect on all the particles of primary concern in this experiment—namely, He, C, N, O, Ne, etc.—because these nuclei all have the same charge to mass ratio and hence the same velocity for a given charge.

To measure the intensity of low-energy heavy nuclei, nuclear emulsions, which are detectors particularly suited for this purpose, were exposed to the cosmic radiation above the earth's atmosphere on a sounding rocket at Fort Churchill, Canada. The use of a sounding rocket rather than a polar orbiting recoverable satellite has several advantages. First, several sounding rocket shots can be spaced at desired intervals, whereas—at least until now—it has not been possible to obtain a single emulsion exposure on a recoverable satellite under less

than about 2 g/cm^2 of material in a region of space where low-energy particles are not excluded by the earth's magnetic field. Also, satellite exposures are very expensive because of the cost of the necessary modifications to an existing system and the cost of testing to meet the rigid design specifications. The design of a satellite system is complicated by the requirement that the emulsions must be protected from high temperatures and still be exposed under very little matter. Further, the fact that the geomagnetic cutoffs are uncertain demands that a time resolution device be included in a satellite experiment to obtain absolute fluxes, since emulsions themselves integrate over time. Finally, the high Van Allen belt radiation background arising from the South Atlantic anomaly is an additional disadvantage associated with a satellite exposure.

To overcome the principal difficulty associated with the sounding rocket exposure—namely, having only a short exposure time available, a large area of emulsion was extended from the side of the payload during the portion of the flight when the rocket was above the atmosphere. The rocket was fired from Fort Churchill, Canada, so that the particles of interest could reach the extended detector at full intensity without having been excluded by the earth's magnetic field.

EXPERIMENTAL PROCEDURE

The nuclear emulsion detectors used in this experiment were 600-micron-thick Ilford G-5 emulsions which were assembled in eighteen packs consisting of eighteen emulsions, 6.5 cm by 9.9 cm, placed on top of each

other and covered with Mylar and black electrical tape to give a water- and light-tight package. Six of these packs were placed in each tray and held in place by means of a small metal lip. A photograph of the emulsion section of the payload is shown in Fig. 1. The trays in turn were kept inside of the payload until 61 seconds after launch of the sounding rocket, at which time extension of the trays was begun. Before reentry and 411 seconds after launch, the retraction of the trays was begun. Extension and retraction each took about 7 seconds. These events and others are indicated in the time-altitude curve in Fig. 2.

The rocket itself was an Aerobee 150, which had the capability of carrying the 171-pound payload of this experiment to an altitude of 151 miles. In addition to the standard Aerobee nose cone, there were two extension sections; the one closest to the rocket was a recovery section, and the other was the section which housed the extension mechanisms for the emulsion trays described in the preceding paragraph. The water-tight housing for the emulsion in the retracted position extended up into the standard nose cone section. In addition, the nose cone itself contained a radar beacon, battery power for the extension and retraction motors, and a telemetry section. Magnetometer data for rocket aspect, data on the extension and retraction of the trays, and rocket parameters including acceleration and chamber pressure were telemetered.

The rocket was launched successfully at 1311 U.T. on September 4, 1963, and all parts of the payload functioned properly. It was a quiet day geophysically[10] and the Mt. Washington neutron monitor counting rate was 2318.[11] The nuclear emulsions were recovered, processed, and found

to be in generally good condition. A total emulsion surface area of 821 cm^2 was available for analysis after elimination of the area held under the tray lips and the immediately adjacent area, where the clear solid angle would have been greatly reduced.

A complete area scan was made under a microscope of the top emulsion of each of the packs, as well as a complete rescan to check scanning efficiency. In the original scans, all tracks which were dark and which either had delta rays or were wider than a track formed by a single line of grains were accepted, regardless of the angle the track made in the emulsion. These tracks were then analyzed by a scientist to separate the slow proton and helium tracks from the partiles with charges greater than 2. At this point, all tracks which were within 20 degrees of the perpendicular to the emulsion were rejected. The method of charge and energy analysis is essentially the same as that used previously in other work and described in detail in a paper by Biswas, Fichtel, and Guss[12] and, therefore, will not be repeated here. Only particles which ended in the emulsion were analyzed. When this work was completed, it was found that the sample of particles, although small, was sufficiently large to permit an actual flux determination rather than simply to set an upper limit.

The calculation of the solid angle of collection involves a number of features which are indicated in Fig. 3. First, there is the restriction on the angle with respect to the plane of the emulsion (called "dip angle") mentioned above, corresponding to section A in the figure. Second, there is a very small solid angle, consisting of tracks of small

dips and azimuthal angles in the emulsion which are closest to the rocket axis, which is excluded because particles would have had to pass through the rocket to enter the emulsion within this solid angle. This solid angle segment varies with position on the surface of the emulsion, but a typical segment labeled "B" is shown in Fig. 3. The final and largest portion of the solid angle which was excluded or partially excluded is made up of those angles which are forbidden to the particles by a combination of their paths along the magnetic field and the earth's atmosphere.

The method of calculating the angle of a particle with respect to the vertical for a given altitude above the earth after the particle has mirrored at a lower altitude has been discussed in an earlier paper by Biswas, Fichtel, and Guss.[12] Although the details are complicated and will not be repeated, the net effect is to increase the angle with respect to the vertical in which particles may arrive from 90 degrees to a larger angle which increases with altitude above the earth. There is only a very small solid angle in which particles pass through a significant amount of atmosphere, but not enough to effectively remove them from consideration. Further, the rocket was not quite vertical but had a small coning angle in addition to its spin about the principal axis; therefore, there was a small variation in the position of the set of angles in the emulsion which are at a given angle with respect to the vertical during the flight. This effect increases somewhat the solid angle in the emulsion in which primary tracks may appear but has essentially no effect on the total solid angle for collecting primary

particles. Some of the curves related to this problem are shown in Fig. 3 near the area marked "C" and are labeled C_1, C_2, and C_3. The explanation of these curves is given in the figure caption. No tracks should have been observed in the shaded area C of the solid angle diagram, and none were.

The effective solid angle is then calculated from the equation

$$\Omega = \iint (f \cdot \cos\theta) \sin\theta \, d\theta \, d\varphi ,$$

where θ is the angle with respect to the perpendicular to the emulsion and φ the azimuthal angle in the emulsion; f is a weighting factor which is 0 in the shaded areas of Fig. 3 where no tracks were accepted and 1 in most of the rest of the area except around C, where it varied between 0 and 1 with position, depending on the fraction of the extended time that the primary particles could reach these angles. The cos θ factor occurs because the emulsion collecting area is a flat surface. Since the area marked "B" in Fig. 3 varies with position on the emulsion surface, Ω varies with position, but only very slightly because of the small contribution of segment B. The collection time also varies slightly with position because of the small, but finite, time required to extend the tray. With all the above factors taken into consideration, the effective primary area—collection time—solid angle factor, called "A Ω T," was 60.7 m^2 sr sec.

The major correction to the raw data is the one which accounts for the background tracks formed during ascent before the trays are extended and during descent after the trays are retracted. In a more recent version of this experiment flown in July 1964, this correction was elimi-

nated by including a sliding plate mechanism which permitted separation of the tracks formed during the period that the emulsion trays were extended from those tracks made at other times. The results of this experiment will be reported later when the data reduction and analysis is complete.

The background consisted of particles of relatively large ambient energies because they had to pass through several g/cm^2 of material before reaching the emulsion, the exact amount of material depending on the angle and the height of the rocket in the atmosphere. An estimate of this background correction therefore could be made from balloon flight data because the particles composing the background had initial energies which were sufficiently great to reach balloon altitudes. For this purpose, the flux and the energy spectrum of low-energy heavy nuclei were measured in the nuclear emulsion plates carried on a balloon flight made from Fort Churchill on July 15, 1963, when the cosmic ray flux level was known to be essentially the same as on September 4, 1963, because the neutron monitor counting rates for these days differed by only 0.2%. The excellent correlation between low-energy cosmic ray intensities and neutron monitor counting rates has been shown previously by McDonald and Webber.[13] In principle, the background correction could be very complex; in practice, a good approximation is obtained by simple summations because the degraded spectrum changes slowly in shape with increasing amounts of material present and, secondly, because the relative times of moving through variable amounts of residual atmosphere and

remaining under a constant amount of a few g/cm^2 of material were about the same for the emulsions in the rocket and those on the balloon.

One final correction which had to be made to the raw data was the increase in the number of collected particles by an amount which took into account the probability that the particles might interact before ending or, in the cases of some of the higher energy particles included in the analysis, leave the stack if it entered the edge at an unfavorable angle. The upper limit to the energy was kept small in order to keep this correction small.

RESULTS AND DISCUSSION

After completion of the analysis outlined in the previous section, the results shown in Table I were obtained. The first point to be made is obvious: namely, that these fluxes are quite clearly significantly different from zero. Hence, a finite flux of cosmic ray medium nuclei in an energy range as low as 30 to 70 MeV/nucleon has been observed in the vicinity of the earth. Further, there is a finite flux of heavy nuclei with energies at least as low as 110 MeV/nucleon.

In the rest of the paper, the heavy nuclei will be divided into two groups—nuclei with nuclear charges from 10 to 19, hereafter called ($10 \leq Z \leq 19$) nuclei, and very heavy nuclei ($Z \geq 20$)—because it is advantageous to keep the variation in energy loss within a charge group to within tolerable limits and because there were very few nuclei with charges of 20 or more. Comments on light nuclei ($3 \leq Z \leq 5$) will be confined to the last paragraph of this section, since they are a separate subject.

The next subject of interest is the comparison of the differential energy spectra obtained in this experiment with the differential spectra at higher energies and with the spectrum of helium nuclei. In this comparison, it is important to remember that the cosmic ray differential energy spectrum varies with the period in the solar cycle. Figure 4 shows the differential energy spectrum for helium for various periods in the solar cycle.[1] The existing data indicate that the medium and heavy nuclei have energy spectra similar to that of the helium nuclei, only reduced in intensity.[1] The medium nuclei group, for example, is 0.063 times the helium particle intensity; and the charge group from Z = 10 to 19 is 0.021 times the helium particle intensity. The possibility of small differences of the order of 15% or less in the region from about 200 to 400 MeV/nucleon cannot be excluded; above 1.5 BeV/nucleon, they probably are correct to within 10%.

At the time of the firing of the sounding rocket from which the data under discussion were obtained, the cosmic ray flux had passed through the minimum value of the cycle a few years earlier and was slowly increasing. The curve in Fig. 5 shows the approximate shape of the helium particle differential spectrum at the time of the rocket shot. It has been shown[1] that the particle spectrum is a smoothly varying function of energy and that for this period in the solar cycle a 1% variation in the Deep River neutron monitor rate, which gives an estimate of the higher energy particle intensity, corresponds to about a 10% variation in the helium particle differential flux at 200 MeV/nucleon. Therefore, for purposes of correlating the measurements made here, an

uncertainty of less than that will be introduced by comparing the results obtained here with helium spectra obtained when the neutron monitor was within 1% of the reading at the time the rocket was in the air. The authors know of four helium spectra in the energy region from about 80 to 600 MeV/nucleon that were obtained during the summer of 1963 which satisfy this condition.[14-17] An average of these spectra, which are in close agreement, was used as the basis for the curve in Fig. 5.

In addition, Fan et al[18] and Ludwig and McDonald[19] have obtained a helium energy spectrum in the 30 to 80 MeV/nucleon region on Explorer XVIII during the period January through March 1964, when the neutron monitor rate was typically from 1 to 2% higher than the rate at the time of the measurement of this experiment. To compensate for a systematic change in intensity in this region, the curve in Fig. 5 was extended below 80 MeV/nucleon by a smooth connection to data above 80 MeV/nucleon, by keeping the shape of the 30 to 80 MeV/nucleon data but reducing the intensity appropriately. This procedure could, at most, introduce a noticeable error only in the lowest medium nuclei energy interval.

Since no comparable data were available for the heavier particles at the time of writing of this paper, the helium particle curve was multiplied by the ratios mentioned abcve to obtain the best possible approximation of the curves for the heavier particles at higher energies.

The results displayed in Figs. 6 and 7 indicate that the low-energy spectrum of the medium nuclei observed in the vicinity of the earth falls below that of the helium nuclei multiplied by 0.063. Similarly, the

($10 \leq Z \leq 19$) nuclei curve falls below the corresponding one for helium nuclei multiplied by 0.021. Hence, the abundance of helium nuclei relative to these higher charge groups apparently increases in the low-energy region until it is well above the fairly constant value which it has from about 400 MeV/nucleon to very high energies.

The spectra which are observed at the earth represent the source spectra after they have passed through interstellar matter and have been modulated within the solar system. Whereas the solar system modulation affects only the intensity of the increment of flux in a given energy interval, interstellar space contains enough material along the path of the particle to change appreciably the particle energy as well as the intensity. In the latter case, it normally is assumed that the intensity is changed significantly only by fragmentation in interactions and not by the complicated time-dependent magnetic effects which cause the intensity variation in the solar system. Therefore, the differential energy flux at the source for the i^{th} type of particle $j_s(i)$ is related to the differential energy flux observed in the vicinity of the earth but outside the region where the earth's magnetic field excludes, or partially excludes, particles $j_o(i)$ by the relation

$$j_o(i)\Big]_{E=E_o} = j_s(i)\Big]_{E=E_s(i)} \left[\frac{\Delta E_s(i)}{\Delta E_o}\right] h(v_o,R) \quad f(i,v,\rho) , \quad (1)$$

where ΔE_o and ΔE_s represent the small energy increments containing the set of particles at the observation point and the source respectively, i is the type of particle, h the solar modulation function, f the

interstellar intensity variation factor, v the particle velocity, R the rigidity (momentum/unit charge), and ρ the amount of interstellar matter traversed between the source and the earth.

The expression $f(i,v,\rho)$ is well known and is given in detail in a paper by Hayakawa.[20] However, the parameters to be substituted into the equations are not known exactly. The parameters include the mean free paths of the different elements in space, the probability of one type of particle emerging from an interaction caused by another particle and the amount of material traversed. Table II gives the values of the parameters used in the calculation and the references from which the parameters were obtained.[21-24] When more than one reference is given, the parameter listed in the Table is a weighted average. In Table II, P_{ij} gives the average number of secondaries of type "j" formed in an interaction of a particle of type "i" in an interaction with a hydrogen nucleus. λ'_i is the absorption mean free path, which is given by the equation

$$\frac{1}{\lambda'_i} = \frac{1}{\lambda_i} (1 - P_{ii}) \quad , \tag{2}$$

where λ_i is the interaction mean free path.

The above parameters are known to vary with energy; however, their exact dependence is not well known. Above approximately 100 MeV/nucleon they are thought to be nearly constant and not to vary appreciably until the energy/nucleon is below about 30 or 60 MeV.[23,25] To reach the earth at the observed energies after passing through several g/cm^2 of interstellar hydrogen, the particles under consideration must spend

either all or almost all of their time in interstellar space at energies above 100 MeV/nucleon. Therefore, it seems reasonable to use the parameters obtained at higher energies in view of the above considerations and the lack of sufficient information to calculate more exact values. Including the generally accepted partially tested hypothesis that the energy per nucleon does not vary significantly in an interaction leads, then, to the conclusion that f is not a function of velocity in the region of interest if ρ is not a function of energy.

The true modulation function h(v,R) is not known. Many models have been presented, and each seems to have some advantages and some weaknesses.[26] For the purposes of the present discussion, it is sufficient to note that, since all the proposed modulation mechanisms involve only magnetic or electric fields and the amount of material traversed within the solar system is negligible, particles with the same charge to mass ratio and hence the same rigidity for a given velocity will be depressed by the same amount for a given velocity.

The remaining term on the right side of Eq. (1), which multiplies $j_s(i,E)$, is $(\Delta E_s(i)/\Delta E_o)$. This term arises from the change in the width of the energy interval in which particles are contained as they lose energy. Since the rate of energy loss per nucleon varies with the nuclear species, this term will affect the different nucleon groups in different ways. Further, because of the different rates of energy loss for a given E_c, $E_s(i)$ will be different for different nuclear species; and hence $j_s(i,E)\Big]_{E=E_s(i)}$ can vary for a fixed E_o even if $j_s(i,E)$ is the same for all nuclear groups.

Consider now the ratio of the differential flux values of two different nuclear types with the same charge to mass ratio. From Eq. (1), this ratio is

$$\frac{j_o(i,E)\big]_{E=E_o}}{j_o(k,E)\big]_{E=E_o}} = \frac{j_s(i,E)\big]_{E=E_s(i)} \quad [\Delta E_s(i)/\Delta E_o]\ f(i,v,\rho)}{j_s(k,E)\big]_{E=E_s(k)} \quad [\Delta E_s(k)/\Delta E_o]\ f(k,v,\rho)} . \tag{3}$$

If ρ, the fragmentation parameters, and the mean free paths are independent of velocity, $f(i,v,\rho)/f(k,v,\rho)$ becomes a constant independent of velocity. Hence,

$$\frac{j_o(i,E)\big]_{E=E_o}}{j_o(k,E)\big]_{E=E_o}} = \frac{j_s(i,E)\big]_{E=E_s(i)} \quad [\Delta E_s(i)/\Delta E_o]}{j_s(k,E)\big]_{E=E_s(k)} \quad [\Delta E_s(k)/\Delta E_o]} \quad \Big[K(\rho,i,k)\Big] \tag{4}$$

$$, \Big[K \neq g(V)\Big]$$

Notice also that

$$\Delta E_s(i)/\Delta E_o \xrightarrow[v \to c]{} 1 \tag{5}$$

and, for reasonable spectra,

$$\Big\{j_s(i,E)\big]_{E=E_s(i)}\Big\} \Big/ \Big\{j_s(k,E)\big]_{E=E_s(k)}\Big\} \xrightarrow[v \to c]{} \text{(Const.), for a fixed E} \tag{6}$$

The implications of the experimental results now will be examined by comparing the data with the predictions based on several suggested source spectra and interstellar mean free paths. If it is assumed first that Eq. (4) is valid, the expected ratio for $j_o(i,E)\big]_{E=E_o}$ and $j_o(k,E)\big]_{E=E_o}$

can be calculated for different values of ρ and the experimental knowledge of the limiting value for the ratio at high energies, where Eqs. (5) and (6) apply.

The most commonly assumed source spectrum is a power law in the total energy with an exponent of 2.5 as given by

$$j_1(i,W) = K_1(i)/W_N^{2.5} \quad , \tag{7}$$

where W_N is the total energy/nucleon. In Figs. 8 and 9 the observed ratios of the differential medium nuclei and the ($10 \leq Z \leq 19$) nuclei to the differential helium nuclei spectral points obtained in the manner described earlier are plotted and compared with the ratio expected on the basis of the observed high-energy ratio and an assumed spectral shape of the form of Eq. (7). The best recent value for the estimate of the amount of interstellar matter traversed—at least for high-energy particles—is 2.5 g/cm^2, which is based on a calculation by Badhwar et al[23] and Badhwar and Daniel[25] with heavy emphasis on the high-energy (> 1.5 BeV/nucleon) composition data of O'Dell et al.[27] The expected ratio has been calculated for both 2.5 and 5.0 g/cm^2 of interstellar hydrogen. Notice that this ratio is relatively insensitive to a change of a factor of 2 in interstellar matter in this range of values. Notice also that the agreement between the experimental points and the curves for these assumed conditions is satisfactory.

As a second example, a source spectrum of the form of Eq. (7) above 300 MeV/nucleon and of the form of Eq. (8) below 300 MeV/nucleon is chosen:

$$j_2(i) = K_2(i)/(E_s)^{0.67} \tag{8}$$

The expected ratios for this source spectrum, the observed high-energy ratios, and 2.5 and 5.0 g/cm^2 of interstellar matter also have been calculated and are shown in Figs. 8 and 9. Here again there is a relatively small difference in the curves for 2.5 and 5.0 g/cm^2, and there is satisfactory agreement with the experimental data. Smooth changes in the source spectrum in general have little effect on the resultant ratios unless the variations are very large, that is, appreciably greater than those selected here.

Hence, the following conclusion can be drawn: The experimentally observed helium to medium and helium to ($10 \leq Z \leq 19$) nuclei ratios are consistent with the assumption that the source spectra are the same and that the particles have passed through the same amount of material, which is in the range of 2.5 to 5 g/cm^2. This conclusion is relatively independent of the exact shape of the source spectrum. On the other hand, differences in the source spectra between helium and medium nuclei would appear relatively quickly in the form of a disagreement between the calculated and observed helium to medium nuclei ratio as a function of energy.

The results obtained here, then, suggest there is good reason to think that above about 0.2 BeV/nucleon the source spectra of all components are at least similar. Information below this energy is not forthcoming from this approach because nuclei of the higher charges being considered must have at least this energy initially to reach the earth.

Next, assume that the particles have gone through different amounts of interstellar material depending on their energy. Dahanayake et al.,[28]

for example, suggest that the lower energy particles, below about 400 MeV/nucleon, have passed through more material than the high-energy ones, which are assumed to go through 2.5 g/cm^2 on the basis of the work mentioned earlier. In this case, $f(i,v,\rho)/f(j,v,\rho)$ of Eq. (3) is not a constant independent of energy. However, if the high-energy ratio of the observed fluxes is known and if the parameters of Table II are used, the additional expected suppression resulting from low-energy particles going through more material than high-energy ones can be calculated. The results obtained, assuming that all particles have a source spectrum of the type given by Eq. (7) and that the particles below 400 MeV/nucleon have passed through 6 g/cm^2 (as suggested by Dahanayake et al.[28]) while the high-energy ones (kinetic energy > 1.5 BeV/nucleon) have passed through 2.5 g/cm^2, are also shown in Figs. 8 and 9. Here the agreement is poorer; further, these assumptions lead to a ratio in the 300 to 400 MeV/nucleon region which is appreciably more than one standard deviation below several measurements of the medium to heavy nuclei ratio in that region. In addition, Hildebrand and Silberberg[29] and Webber[30] now have shown that the existing experimental data on the He_3/He_4 ratio probably can be reconciled with a mean free path in the low-energy region which is the same or only slightly larger than 2.5 g/cm^2, by taking into account the properties of secondaries from interactions and the effects of the solar modulation mechanism on particles with different charge to mass ratios.

Light nuclei also were observed in the low-energy region from 30 to 110 MeV/nucleon, but no quantitative value for the differential flux will

be quoted because a high scanning detection efficiency was not achieved for these particles. Since these light nuclei generally are assumed to arise from heavier nuclei, the type of theoretical analysis outlined above does not apply. There is, however, the alternate problem of interest: namely that, if the modulation effect is rigidity dependent, light nuclei might be expected to have slightly different energy spectra from the medium or heavy nuclei. If the rigidity dependence of the modulation can be determined by other means, the relative abundance of light and medium nuclei provide an independent estimate of the amount of interstellar matter traversed by the cosmic radiation at these low energies. The analysis was not pressed beyond the determination of the existence of a light nuclei flux because there was not an adequate number of particles to determine the light to medium ratio with sufficient accuracy to see a deviation from the high-energy ratio; and the additional work involved is tremendous. With an improved technique and a higher flux rate, we hope to be able to measure the relative abundance of light nuclei in the 1964 flight to be reported later.

CONCLUSIONS

The answer to the basic question of whether or not there are low-energy heavy nuclei below the energy cutoff set by material above detectors flown on balloons has been seen to be "Yes." There definitely is a finite flux of medium nuclei in an energy range as low as 30 to 70 MeV/nucleon and ($10 \leq Z \leq 19$) nuclei with energies at least as low as 110 MeV/nucleon. The abundances of medium and ($10 \leq Z \leq 19$) nuclei relative to helium nuclei in the energy regions from 30 to 150 and 30 to 190 MeV/nucleon,

respectively, are less than the relative abundances at higher energies. This difference can be explained quantitatively by the higher rate of energy loss of the particles of higher charge in the interstellar matter. It also was shown that within the statistical uncertainty the resulting differential flux measurements are consistent with the helium, medium, and ($10 \leq Z \leq 19$) nuclei having the same source spectrum at least above about 0.2 BeV/nucleon for a wide range of source spectral shapes, including ones normally assumed. For a mean free path independent of energy this result also is fairly insensitive to the values of cross sections and fragmentation parameters assumed, principally because relative values of ratios are being considered. The conclusion is independent of the solar modulation mechanism because, since all particles considered have the same charge to mass ratio, their relative abundances at a given velocity will be unaffected by the local solar modulation. No information can be obtained about the source spectrum below about 0.2 BeV/nucleon because the particles of high charge must have approximately this energy to reach the earth after passing through interstellar matter.

It has been established that there is a finite flux and that the differential flux is consistent with similar source spectra for helium, medium, and heavier nuclei and an interstellar path in hydrogen of 2.5 g/cm^2 within the relatively large uncertainties of these initial measurements. It now seems worthwhile to measure these spectra again to look for a possible variation with the period in the solar cycle and to examine the matters discussed in this paper in greater detail. This problem is being pursued.

Table I. Differential fluxes for medium nuclei and ($10 \leq Z \leq 19$) nuclei on September 4, 1964.

Kinetic energy (MeV/nucleon)	$6 \leq Z \leq 9$ [p/(m² sr sec MeV/nucleon)]	$10 \leq Z \leq 19$ [p/(m² sr sec MeV/nucleon)]
50	0.0040 ± 0.0015	-
55	-	0.0005 ± 0.0006
90	0.0055 ± 0.0018	0.0005 ± 0.0006
130	0.0072 ± 0.0024	0.0040 ± 0.0015
170	Not measured	0.0028 ± 0.0014

Table II. Parameters used for extrapolation through interstellar matter.

	Reference		References
$\lambda_\alpha = 14.6$ g/cm^2	20	$P_{\alpha\alpha} = 0.07 \pm 0.07$	21-24
$\lambda_M = 6.0$ g/cm^2	20	$P_{(L+M+H)\alpha} = 1.3 \pm 0.5$	21-24
$\lambda_H = 4.0$ g/cm^2	20	$P_{MM} = 0.14 \pm 0.04$	21-24
		$P_{HM} = 0.21 \pm 0.10$	21-24
		$P_{HH} = 0.40 \pm 0.15$	21-24

[15]C. E. Fichtel, D. E. Guss, D. A. Kniffen, and K. A. Neelakantan, work to be submitted to Phys. Rev.

[16]J. Ormes and W. R. Webber, Phys. Rev. Letters 13, 106 (1964).

[17]P. S. Freier and C. J. Waddington, Phys. Rev. Letters 13, 108 (1964).

[18]C. Y. Fan, G. Gloeckler, and J. A. Simpson, Trans. Am. Geophys. Union, Vol. 45, 8 Sept. 1964.

[19]G. H. Ludwig and F. B. McDonald, to be submitted for publication in Phys. Rev. Letters.

[20]S. Hayakawa, Progr. Theoret. Phys. (Kyoto) 15, 111 (1956).

[21]M. W. Friedlander, K. A. Neelakantan, S. Tokunaga, G. R. Stevenson, and C. J. Waddington, Phil Mag 8, 1691 (1963).

[22]H. Aizu, Y. Fujimoto, S. Hasegawa, M. Koshiba, T. Mitto, J. Nishimura, and K. Yokoi, Progr. Theoret. Phys. (Kyoto), Suppl. 16 (1960).

[23]G. D. Badhwar, R. R. Daniel, and B. Vijayalakshmi, Progr. of Theoret. Phys. (Kyoto) 28, 607 (1962).

[24]S. Hayakawa, K. Ito and Y. Terashima, Progr. Theoret. Phys. (Kyoto), Suppl. 6, 1 (1958).

[25]G. D. Badhwar and R. R. Daniel, Progr. Theoret. Phys. (Kyoto) 30, 613 (1963).

[26]For a discussion of this problem see, for example, Ref. 9 or C. E. Fichtel, D. E. Guss, G. R. Stevenson and C. J. Waddington, Phys. Rev. 133, B818 (1964).

[27]F. W. O'Dell, M. M. Shapiro, and B. Stiller, J. Phys. Soc. Japan 17, Suppl. A-III, 23 (1962).

List of Footnotes

*NAS-NASA Research Fellow, on leave from Tata Institute of Fundamental Research, Bombay, India.

[1]W. R. Webber, Progress in Elementary Particle and Cosmic Ray Physics VI (North Holland Publishing Co., Amsterdam) p. 77 (1962).

[2]Proceedings of the International Conference on Cosmic Rays, Jaipur, India, Commercial Printing Press Limited, Bombay (1963).

[3]Proceedings of the International Conference on Cosmic Rays and the Earth Storm, Kyoto, 1961, J. Phys. Soc. Japan 17, Suppl. A-III (1962).

[4]H. Aizu, Y. Fujimoto, S. Hasegawa, M. Koshiba, I. Mito, J. Nishimura, and K. Yokoi, J. Phys. Soc. Japan 17, Suppl. A-III, 38 (1962).

[5]D. E. Evans, Nuovo Cimento 27, 394 (1963).

[6]F. Foster and A. Debenedetti, Nuovo Cimento 28, 1190 (1963).

[7]C. Fichtel, Nuovo Cimento 19, 1100 (1961).

[8]F. B. McDonald and W. R. Webber, J. Geophys. Res. 67, 2119 (1962).

[9]See, for example, F. B. McDonald and W. R. Webber, J. Geophys. Res. 69, 3097 (1964).

[10]J. Virginia Lincoln, J. Geophys. Res. 69, 525 (1964).

[11]Courtesy of the Enrico Fermi Institute for Nuclear Studies, Chicago.

[12]S. Biswas, C. E. Fichtel, and D. E. Guss, Phys. Rev. 128, 2756 (1962).

[13]F. B. McDonald and W. R. Webber, J. Phys. Soc. Japan 17, Supp A2, 428 (1962).

[14]V. K. Balasubrahmanyan and F. B. McDonald, J. Geophys. Res. 69, 3289 (1964).

[28]C. Dahanayake, M. F. Kaplon, and P. J. Lavakare, J. Geophys. Res. 69, 3681 (1964).

[29]B. Hildebrand and R. Silberberg, Regional IQSY Symposium, Buenos Aires, Aug. 3-8, 1964.

[30]W. R. Webber, Regional IQSY Symposium, Buenos Aires, Aug. 3-8, 1964.

Figures

Fig. 1. Photograph of the rocket payload section with the emulsions removed and the emulsion trays extended. Six emulsion packs were placed in each of three symmetrically positioned trays. The angle of the trays with respect to the rocket axis was 17.5 degrees.

Fig. 2. Rocket time-altitude trajectory, showing the sequence of events: (1) rocket burnout (2) emulsion tray extension (3) emulsion tray retraction (4) payload separation (5) parachute deployment and SARAH beacon activation.

Fig. 3. Distribution of ending $Z \geq 6$ nuclei (indicated by black circles) in the solid angle of collection. The "dip angle" is the angle with respect to the plane of the emulsion; the "azimuthal angle" is that with respect to the perpendicular to one of the edges of the emulsion measured in the emulsion plane. The shaded area "A" was excluded from analysis because tracks in this segment had a dip too great to be analyzed. The shaded area "B" was excluded from analysis because particles at these angles had passed through the rocket material before entering the emulsion; this area varied with position in the emulsion and a typical segment is shown. The curves C_1, C_2, and C_3 are the curves for particles with space angles

Figures (continued)

Fig. 3. (cont'd) greater than 90°, 70°, and 60° with respect to the magnetic line of force. These curves varied somewhat as the coning angle of the rocket varied, and the ones shown are typical. The shaded area "C" is forbidden to the low-energy heavy nuclei under consideration because they would be stopped by ionization energy loss in the atmosphere between the rocket and their mirror point.

Fig. 4. Differential energy spectrum for helium nuclei at various times during the solar cycle. These curves were calculated from data published by Webber (see Ref. 1).

Fig. 5. Helium nuclei differential energy spectrum obtained as explained in the text. The low-energy points, from which the low-energy portion of the curve was deduced, are those of Fan et al. (Ref. 18) and Ludwig and McDonald (Ref. 19).

Fig. 6. Differential energy spectrum for medium nuclei. The curve is that for helium nuclei (Fig. 5) multiplied by 0.063.

Fig. 7. Differential energy spectrum for ($10 \leq Z \leq 19$) nuclei. The curve is that for helium nuclei (Fig. 5) multiplied by 0.021. For the two lowest energy points, only the upper limit corresponding to one standard deviation is shown.

FIGURES (continued)

Fig. 8. Ratio of the differential flux of medium nuclei to helium nuclei expected after passage of the particles through various amounts of interstellar gas. Curve A: 0 g/cm^2 for all spectral shapes; curve $B_{2.5}$ and curve B_5: 2.5 g/cm^2 and 5.0 g/cm^2, respectively, assuming the source spectrum of Eq. (7); curve $C_{2.5}$ and curve C_5: 2.5 g/cm^2 and 5.0 g/cm^2, respectively, assuming the source spectrum of Eq. (7) for particles with kinetic energy greater than 300 MeV/nucleon and the source spectrum of Eq. (8) for particles with kinetic energy less than 300 MeV/nucleon; curve D: passage through 2.5 g/cm^2 for relativistic particles, 6 g/cm^2 for particles with kinetic energy less than 400 MeV/nucleon, assuming the source spectrum of Eq. (7).

Fig. 9. Ratio of the differential flux of ($10 \leq Z \leq 19$) nuclei to helium nuclei expected after passage of the particles through various amounts of interstellar gas. Curve A: 0 g/cm^2 for all spectral shapes; curve $B_{2.5}$ and curve B_5: 2.5 g/cm^2 and 5.0 g/cm^2, respectively, assuming the source spectrum of Eq. (7); curve $C_{2.5}$ and curve C_5: 2.5 g/cm^2, and 5.0 g/cm^2, respectively, assuming the source spectrum of Eq. (7) for particles with kinetic energy greater than

FIGURES (continued)

Fig. 9. (cont'd) 300 MeV/nucleon and the source spectrum of Eq. (8) for particles with kinetic energy less than 300 MeV/nucleon; curve D: passage through 2.5 g/cm^2 for relativistic particles, 6 g/cm^2 for particles with kinetic energy less than 400 MeV/nucleon, assuming the source spectrum of Eq. (7).

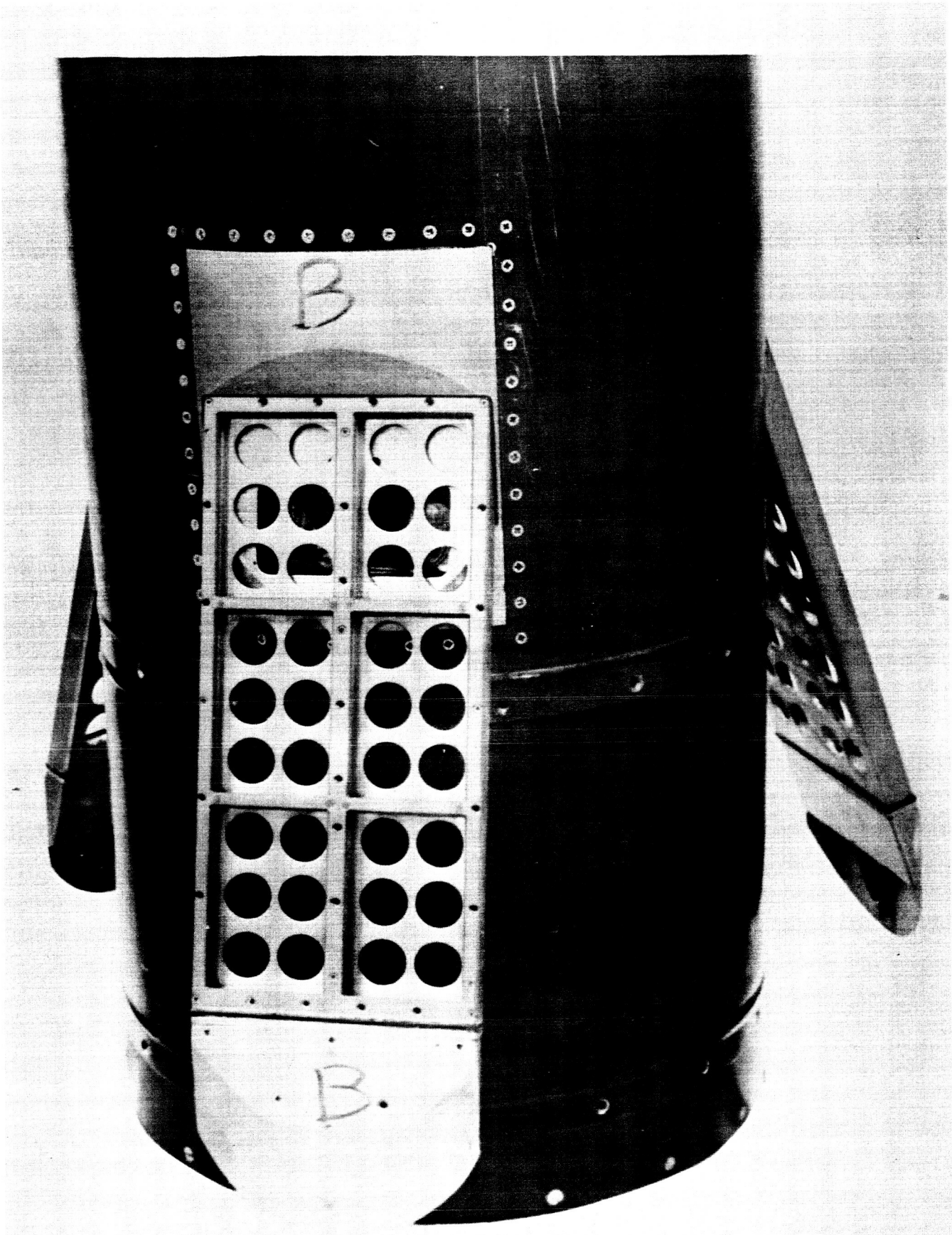

Figure 1

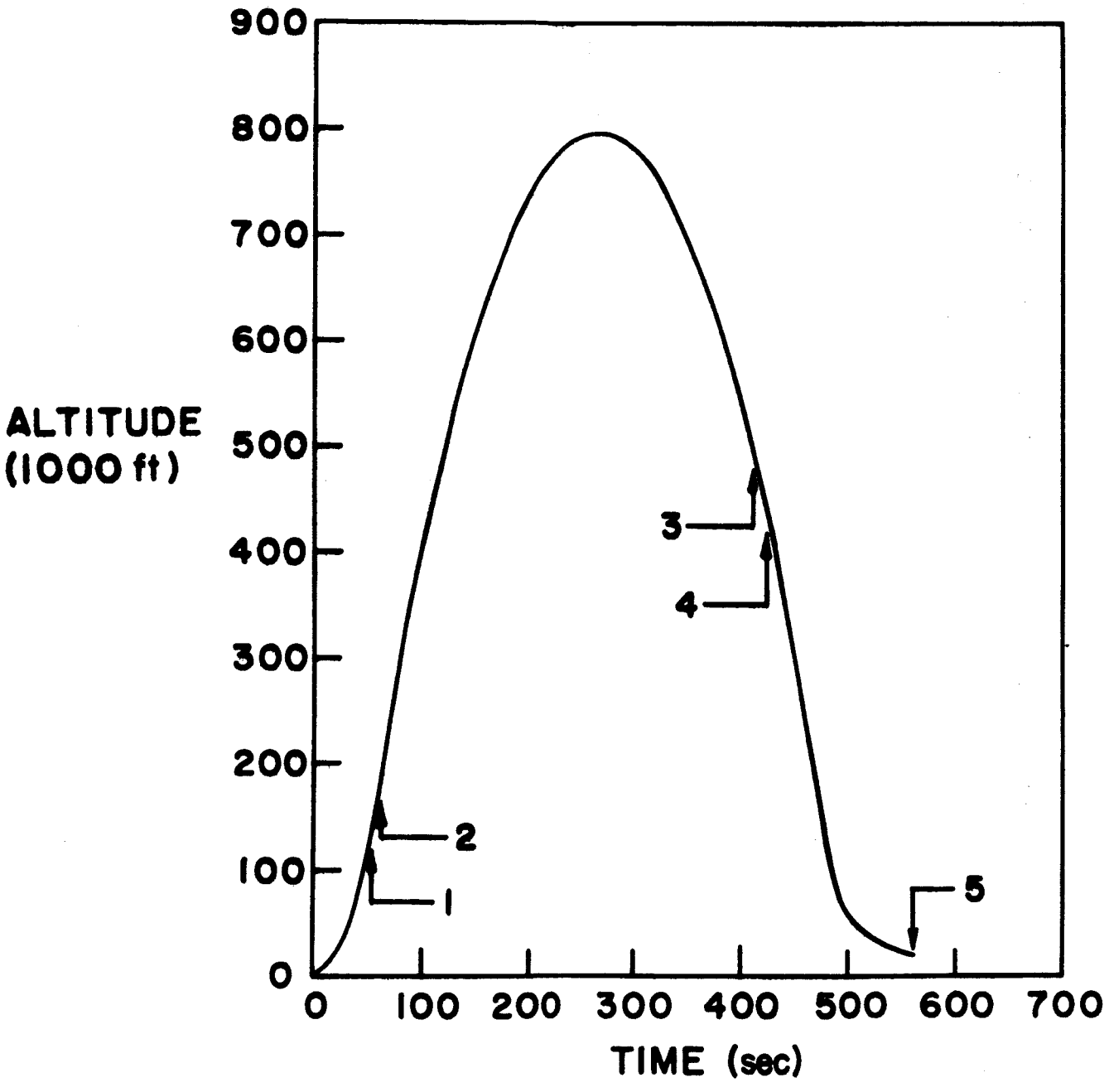
ALTITUDE
(1000 ft)
900
800
700
600
500
400
300
200
100
0
0
100
200
300
400
500
600
700
TIME (sec)
1
2
3
4
5

Figure 2

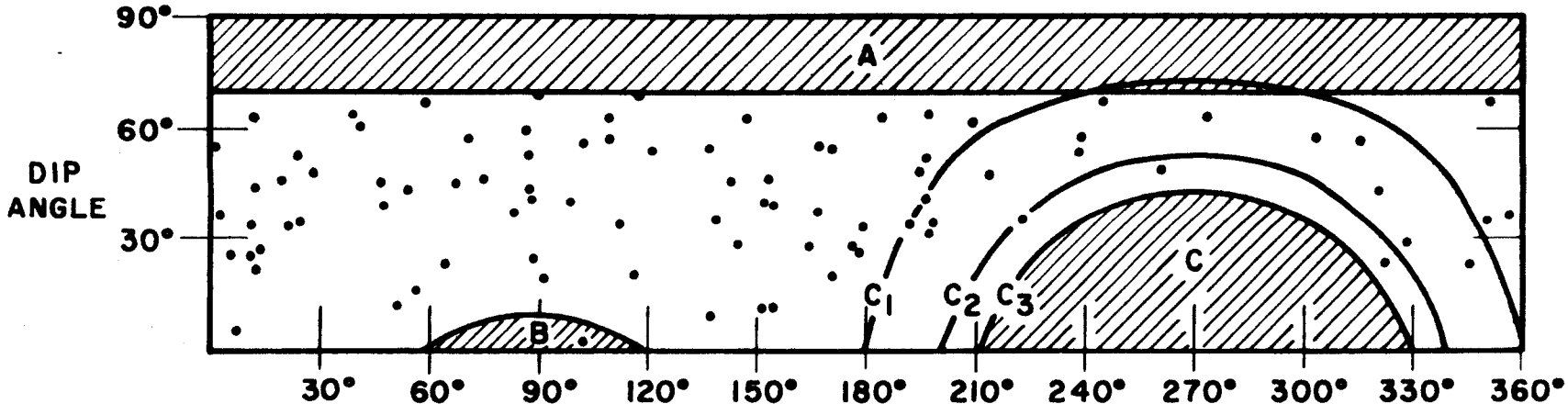
90°
60°
30°
DIP
ANGLE
A
B
C
C1
C2
C3
30°
60°
90°
120°
150°
180°
210°
240°
270°
300°
330°
360°
AZIMUTHAL ANGLE

Figure 3

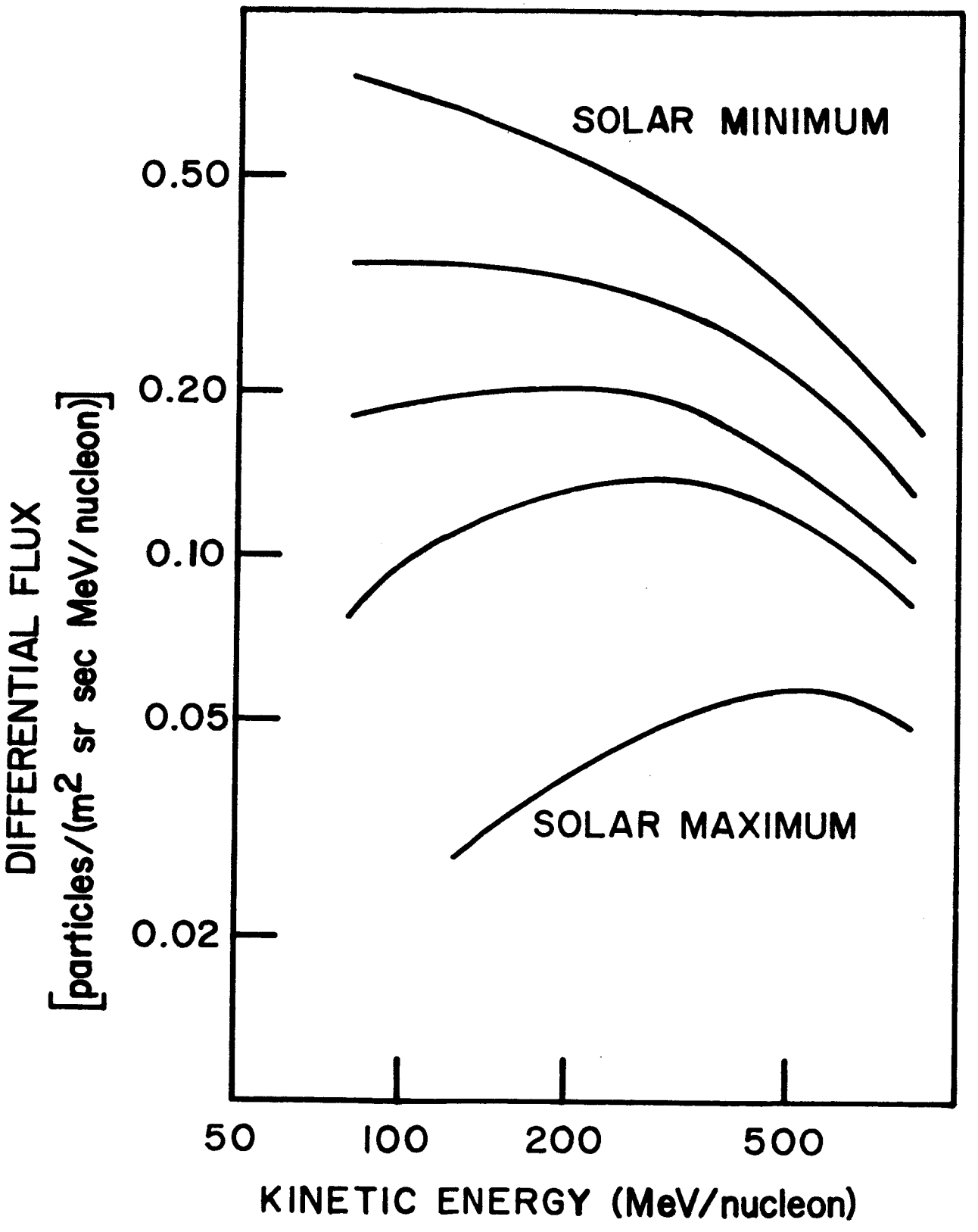
SOLAR MINIMUM
SOLAR MAXIMUM
0.50
0.20
0.10
0.05
0.02
DIFFERENTIAL FLUX
[particles/(m² sr sec MeV/nucleon)]
50
100
200
500
KINETIC ENERGY (MeV/nucleon)

Figure 4

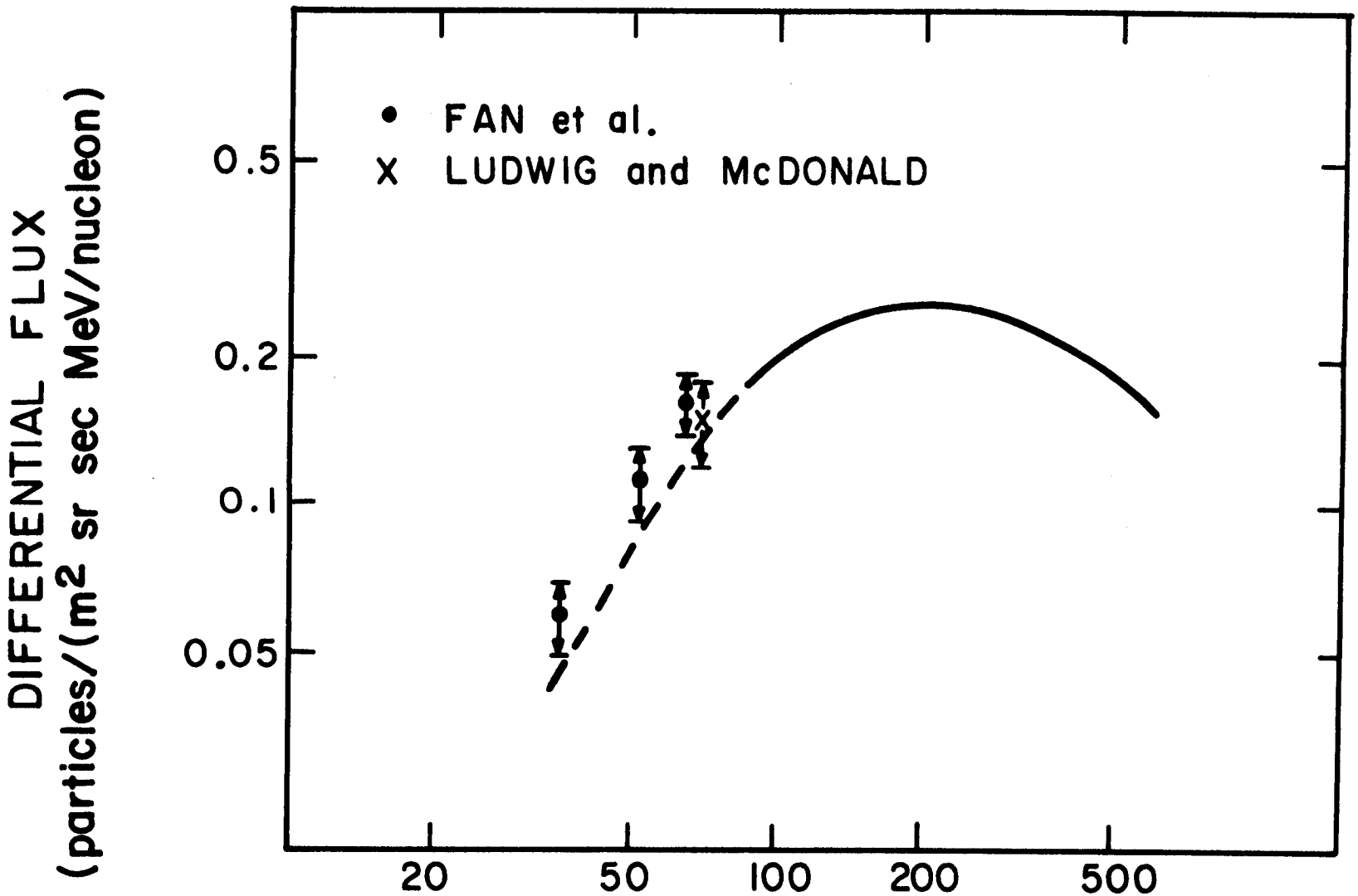
DIFFERENTIAL FLUX
(particles/(m² sr sec MeV/nucleon)
• FAN et al.
X LUDWIG and McDONALD
0.5
0.2
0.1
0.05
20
50
100
200
500
KINETIC ENERGY (MeV/nucleon)

Figure 5

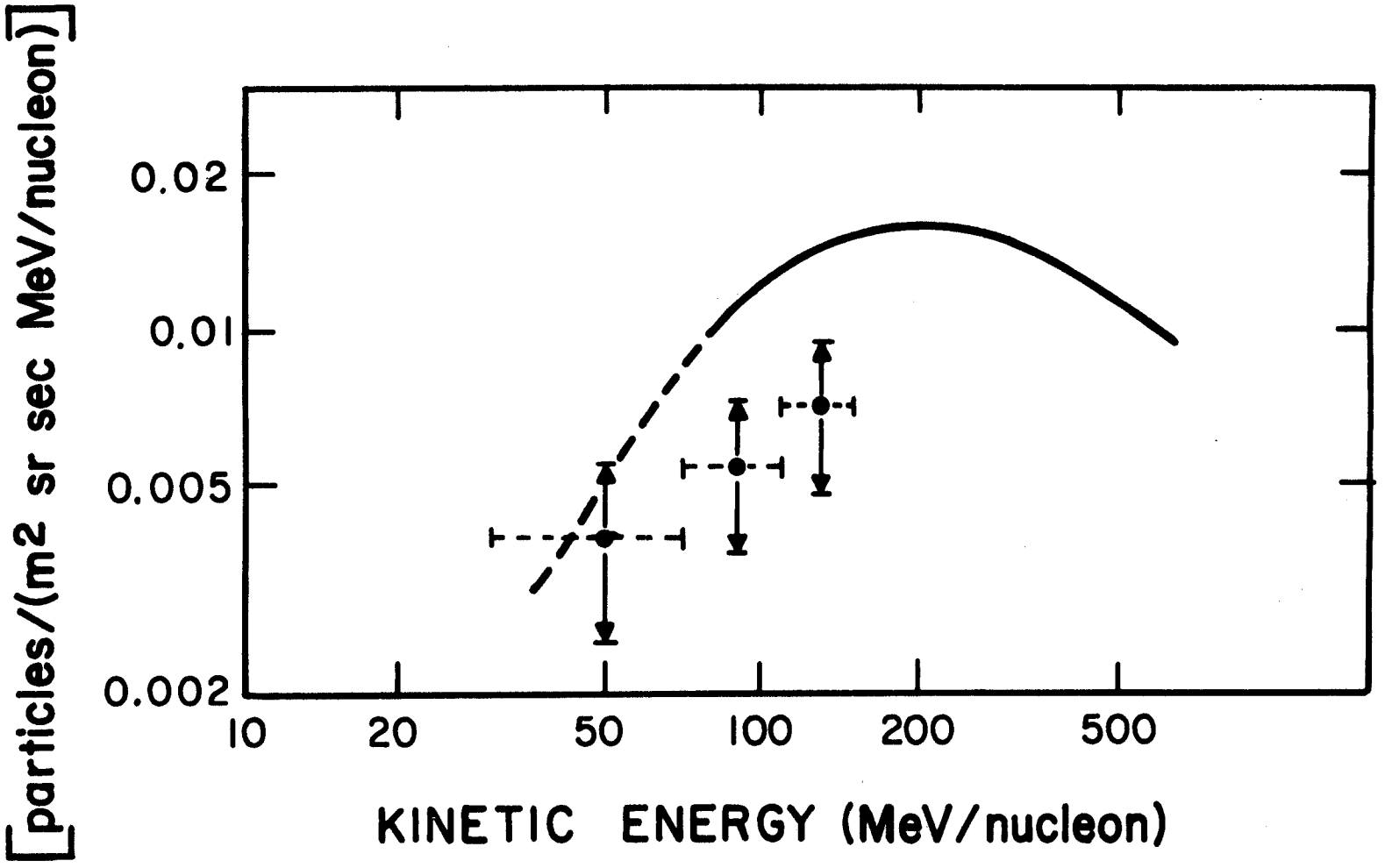
DIFFERENTIAL FLUX
[particles/(m2 sr sec MeV/nucleon)]
0.02
0.01
0.005
0.002
10
20
50
100
200
500
KINETIC ENERGY (MeV/nucleon)

Figure 6

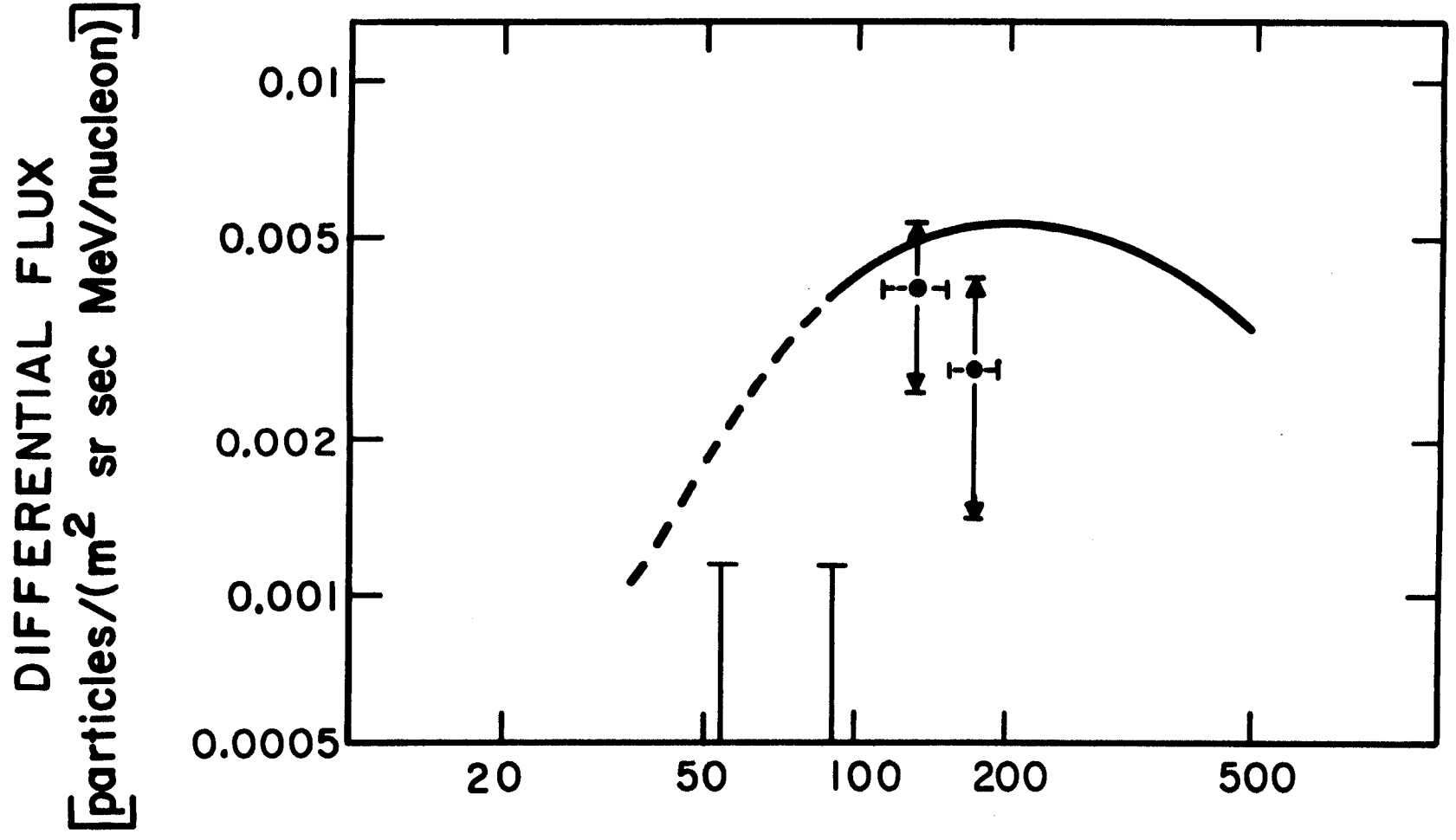
DIFFERENTIAL FLUX
[particles/(m² sr sec MeV/nucleon)]
0.01
0.005
0.002
0.001
0.0005
20
50
100
200
500
KINETIC ENERGY (MeV/nucleon)

Figure 7

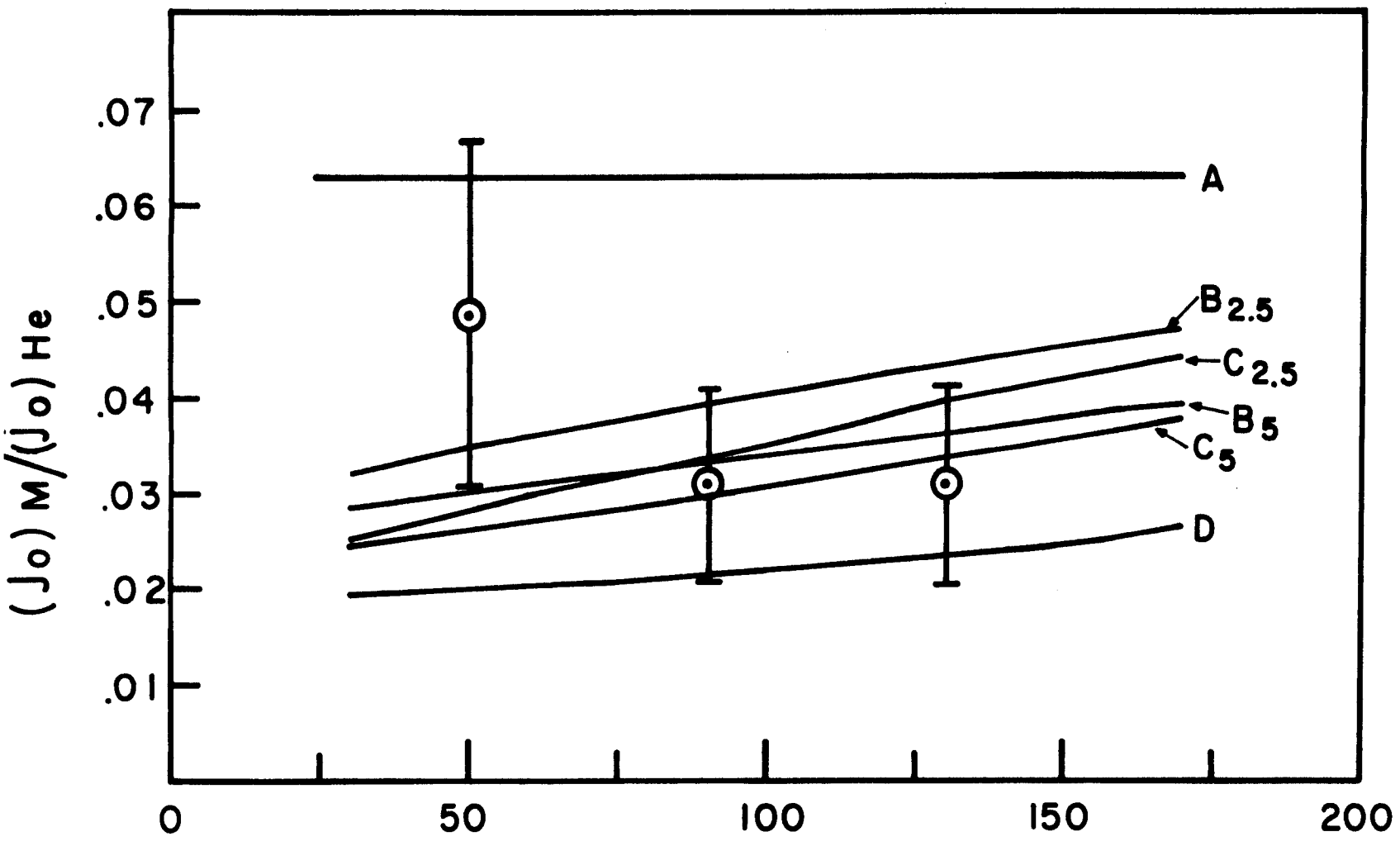
.07
.06
.05
.04
.03
.02
.01
(Jo) M/(Jo) He
A
B2.5
C2.5
B5
C5
D
0
50
100
150
200
KINETIC ENERGY (MeV/nucleon)

Figure 8

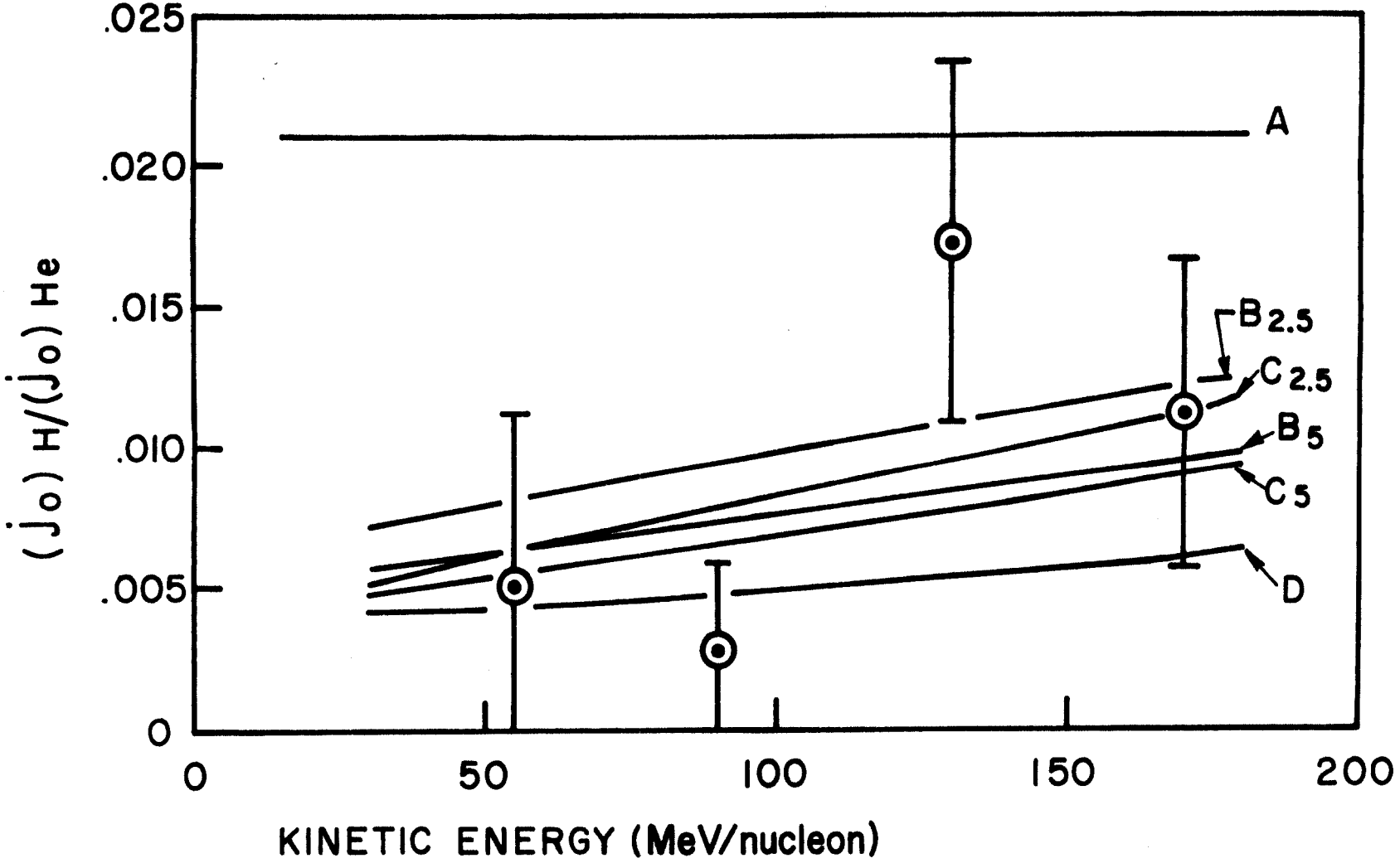
.025
.020
.015
.010
.005
0
0
50
100
150
200
(J₀) H/(J₀) He
KINETIC ENERGY (MeV/nucleon)
A
B2.5
C2.5
B5
C5
D

Figure 9